Research Article | Vol. 27, No. 5 | 4 Mar 2019 | OPTICS EXPRESS 6970
Optics EXPRESS

Fast electrons interacting with a natural hyperbolic medium: bismuth telluride

PRASHANT SHEKHAR,[1,2] SARANG PENDHARKER,[3] DOUGLAS VICK,[4] MAREK MALAC,[4] AND ZUBIN JACOB[1,2,*]

[1]*Department of Electrical and Computer Engineering, University of Alberta, Edmonton, Canada*
[2]*Birck Nanotechnology Center, Purdue University, West Lafayette, IN, USA*
[3]*Dept. of Electronics & Electrical Comm. Eng., IIT Kharagpur, W. Bengal, India*
[4]*Nanotechnology Research Centre, Nat. Res. Council, Alberta, Canada*
[*]*zjacob@purdue.edu*

Abstract: Fast electrons interacting with matter have been instrumental for probing bulk and surface photonic excitations including Cherenkov radiation and plasmons. Additionally, fast electrons are ideal to investigate unique bulk and longitudinal photonic modes in hyperbolic materials at large wavevectors difficult to probe optically. Here, we use momentum-resolved electron energy loss spectroscopy (k-EELS) to perform the first experimental demonstration of high-k modes and hyperbolic Cherenkov radiation in the natural hyperbolic material Bi_2Te_3. This work establishes Bi_2Te_3 as one of the few viable natural hyperbolic materials in the visible and paves the way for k-EELS as a fundamental tool to probe hyperbolic media.

1. Introduction

Fast electrons interacting with matter have been a cornerstone for understanding and discovering new photonic phenomena such as surface plasmons by Ritchie [1] and the generation of Cherenkov as well as Smith-Purcell radiation [2]. In contrast to propagating light waves, the inherent field of a swift electron is evanescent and spectrally broadband and thus probes nanophotonic excitations across a wide range of the EM spectrum well beyond the light cone [3, 4].

Recently using fast electron probes, Shekhar et al. demonstrated metallic and plasmonic properties of silicon thin films (60nm) in the extreme ultraviolet (EUV) [5]. Specifically, using momentum-resolved electron energy loss spectroscopy (k-EELS), plasmonic excitations at EUV energy scales were measured in silicon which is a well-known semiconductor. This paves the way for the field of EUV plasmonics with silicon. One specific application is the use of swift electrons to generate thresholdless Cherenkov radiation in the EUV using silicon based hyperbolic metamaterials (HMMs) [5].

Fast electron sources are also ideal for probing the fundamental excitations of HMMs that support unique nanophotonic modes in the bulk of their structure. A swift electron passing through matter can probe the entirety of the bulk of the HMM unlike traditional photonic sources. Additionally, a swift electron possesses inherent longitudinal fields (alongside its transverse fields) that couple to longitudinal modes of the structure difficult to probe optically. Thus, electrons can probe bulk transverse, longitudinal, and coupled longitudinal-transverse photonic properties of HMMs including high-k modes [6], anomalous scaling laws in HMM nano-cavities [7], super-Coulombic interactions [8], and thresholdless Cherenkov radiation [5, 9, 10].

Naturally occurring hyperbolic materials, composed of "individual layers" on the atomic scale, have been seen to curtail the limitations of the finite size of the unit cell prevalent in artificial hyperbolic structures. As the constituent components of such media are orders of magnitude smaller than the wavelength (such as hBN in the infrared [11, 12] and graphite in the UV [13, 14]), it can be treated as a true effective hyperbolic medium [15–17]. Additionally, recent ellipsometry measurements have shown that the tetradymite Bi_2Te_3, which is also a topological insulator,

#355225 https://doi.org/10.1364/OE.27.006970
Journal © 2019 Received 12 Dec 2018; revised 10 Feb 2019; accepted 12 Feb 2019; published 25 Feb 2019

Optics EXPRESS

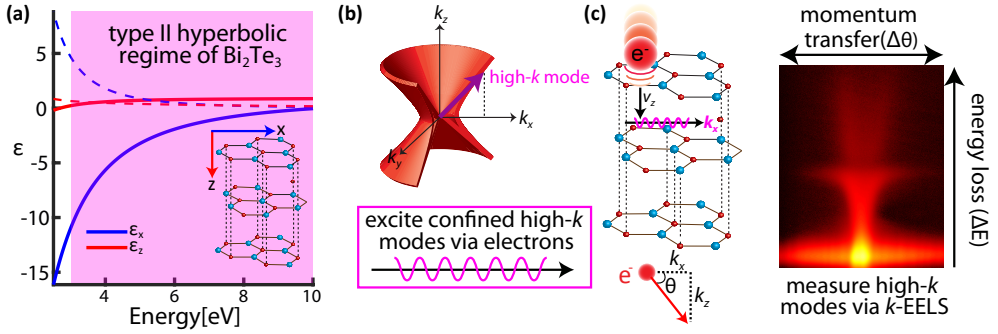

Fig. 1. (a) Uniaxial dielectric permittivity of Bi_2Te_3 parallel (ϵ_z) and perpendicular (ϵ_x) to the c-axis showing type II hyperbolic behaviour ($\epsilon_x < 0$, $\epsilon_z > 0$) in the visible to the UV. Note the estimated plasma frequency of the ϵ_z component is blue shifted by 1.5 eV compared to [18] as a parameter fit to our experimental data. (b) The type II hyperbolic isofrequency surface of Bi_2Te_3 that can support photonic excitations with large momentum (high-k modes) that would normally decay in conventional media. (c) Schematic showing the excitation of high-k modes in Bi_2Te_3 via fast electrons. The subsequent energy loss (ΔE) and scattering angle (θ) of the electron as it passes through the sample is measured and corresponds directly to the energy and momentum (k) of the excited modes in the structure.

possesses hyperbolic behaviour in the visible [18]. The strong anisotropy is clearly evident in the uniaxial dielectric permittivity of Bi_2Te_3 parallel (ϵ_z) and perpendicular (ϵ_x) to the crystal axis shown in Fig. 1(a) (parameter fit is used for ϵ_z, see figure caption). Bi_2Te_3 has a characteristic type II hyperbolic isofrequency response ($\epsilon_x < 0$, $\epsilon_z > 0$) (Fig. 1(b)). Bi_2Te_3 and Bi_2Se_3 are the only known naturally occurring materials to exhibit hyperbolic behaviour in the visible [15, 18].

In this paper, we use k-EELS to perform the first experimental measurements of the high-k modes in Bi_2Te_3 and confirm its natural hyperbolic character from the visible to the UV. The k-EELS technique uses relativistic electrons with high energy and momentum that are able to couple to Bi_2Te_3's large momentum (high-k) states that are difficult to probe optically (Fig. 1(c)). Unlike more traditional spatially resolved electron energy loss techniques, both the energy and the momentum dispersion of the high-k modes are measured. Alongside optical excitations, electron spectroscopy techniques can also probe photonic excitations generated by fast moving charges, such as Cherenkov radiation (CR). Here, with k-EELS, we show the first measurement of hyperbolic CR in a natural hyperbolic material (Bi_2Te_3) and discuss its unique thresholdless CR properties. We corroborate our experimental results using macroscopic electron energy loss theory. This work paves the way for realizing Bi_2Te_3 as a viable natural hyperbolic material from the visible to UV through its ability to support high-k modes and thresholdless CR. Furthermore, we establish k-EELS as a fundamental tool to probe high-k excitations in any hyperbolic media.

2. Electron scattering probability of Bi_2Te_3 in the hyperbolic regime

Probing optical excitations in nanophotonic structures with electrons has been conducted with a variety of techniques such as cathodoluminescence, photoemission electron microscopy, and EELS [2]. In k-EELS, relativistic electrons normally incident on a sample will lose a characteristic amount of energy (ΔE) and be scattered at a particular scattering angle (θ) which corresponds directly to the energy and the momentum (k) of excitations supported by the sample (Fig. 1(c)). The predicted energy loss and scattering angle of the electron in experiment can be calculated via the semi-classical electron energy loss probability [19, 20]. Additionally, the energy loss probability has been shown to be closely related to the photonic density of states [2, 21].

Figure 2 (a) shows the simulated momentum-resolved electron energy loss probability for a

Optics EXPRESS

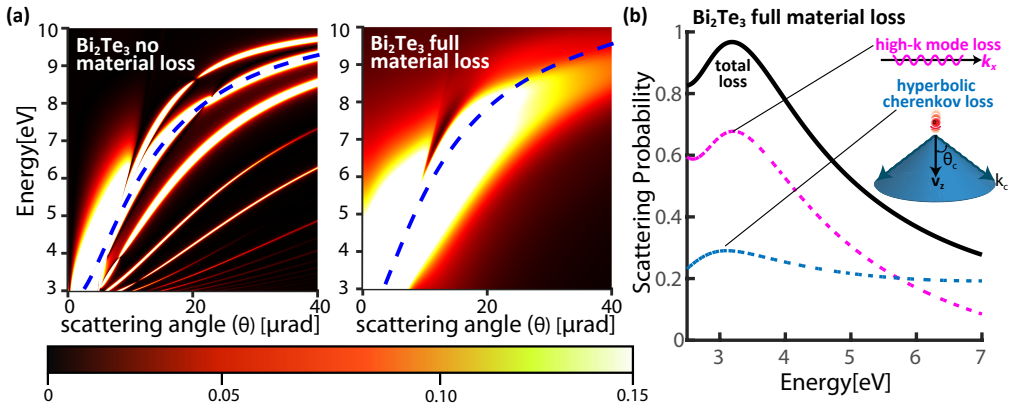

Fig. 2. (a) The calculated total momentum-resolved electron energy loss probability in a 60 nm thick Bi_2Te_3 film with electrons impinging normal to the sample interface with a velocity $v_z = 0.78c$. In the case of Bi_2Te_3 with no material damping (left) a series of dispersive bands are observed corresponding to the high-k modes of the structure. In the case with full material damping (right) dampening and broadening of the high-k modes is seen. The dashed blue line is the analytic dispersion of the hyperbolic CR mode (Eq. (1)) excited in the sample alongside the high-k modes. (c) The theoretical electron energy loss probability integrated over the scattering angle (θ) showing the total loss as well as the individual contributions to the loss spectrum from high-k modes and hyperbolic CR.

60 nm thick Bi_2Te_3 film with electrons normally incident on the structure with a velocity of $v_z = 0.78c$ with (right) and without (left) material damping. Note that Fig. 2(a) is a representation of the photonic bandstructure of Bi_2Te_3 in the hyperbolic regime as $\theta \propto k$. For the case of no material damping, the dispersion profiles for a series of bands is apparent in the $3 - 9.5$ eV ($\approx 130 - 410$ nm) range which are the characteristic type II hyperbolic high-k modes. However, Bi_2Te_3 is highly lossy in the hyperbolic regime [15] and, with regular material damping, the individual high-k mode dispersions become broadened and damped (Fig. 2(a) (right)).

In addition to the high-k modes, electrons in k-EELS also excite CR in Bi_2Te_3. CR is electromagnetic radiation generated when a moving charged particle passes through a medium with a velocity greater than the phase velocity of light in the medium $v_{particle} \geq c/\sqrt{\epsilon}$ [20,22,23]. CR in a uniaxial structure such as Bi_2Te_3 is emitted in the shape of a cone (Fig. 2(inset)) with a Cherenkov cone angle (θ_c) described by the dispersion:

$$tan(\theta_c) = k_c^x/k_c^z = \sqrt{(v_z/c)^2\,\epsilon_z - \epsilon_z/\epsilon_x} \tag{1}$$

where v_z is the electron velocity and k_c^x and k_c^z are components of the Cherenkov wavevector k_c [5, 19]. The CR dispersion is plotted in Fig. 2(a) as the dashed blue line and exists in the hyperbolic regime of Bi_2Te_3 (hyperbolic CR).

The total loss probability of Bi_2Te_3 in the hyperbolic regime is thus predominately composed of contributions from high-k modes and hyperbolic CR. This is seen in Fig. 2(c) which plots the total integrated scattering probability (black line) alongside the isolated contributions from high-k modes and the hyperbolic CR mode. Hyperbolic CR is a coherent effect across the bulk of the structure and thus has a relatively lower scattering probability in a thin 60 nm film.

Recently, it has been shown that hyperbolic CR eliminates the need for high velocity electrons required for CR generation in conventional dielectrics [5, 9, 10, 24]. In fact, in the ideal limit, CR in a type II hyperbolic material can be generated for an electron traveling with any velocity ($0 \leq v_z \leq c$), known as thresholdless Cherenkov radiation (TCR) (Fig. 3(a)). The foundation of

Optics EXPRESS

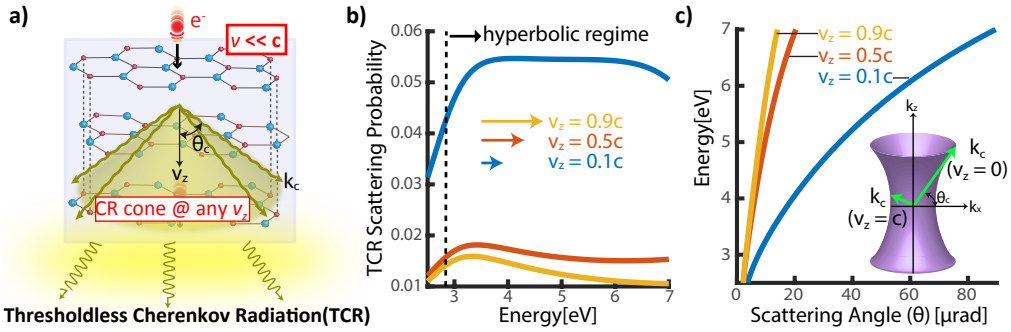

Fig. 3. (a) Schematic showing the generation of thresholdless Cherenkov radiation (TCR) in Bi_2Te_3 in the hyperbolic regime with a Cherenkov cone angle θ_c and Cherenkov wavevector k_c. (b) Calculated electron scattering probability integrated over the scattering angle for TCR in a 60 nm Bi_2Te_3 film (with regular material damping) for normally incident electrons with different velocities. (c) Analytic TCR dispersion profiles (Eq. (1)) for a 60 nm Bi_2Te_3 film at different electron velocities. The TCR dispersion extends to larger scattering angles (higher k) for the slower electrons due to the unique hyperbolic dispersion (inset).

the TCR phenomena is due to the unique hyperbolic topology of the isofrequency surface. In a type II hyperbolic material ($\epsilon_z > 0, \epsilon_x < 0$), if we take the limit $v_z \rightarrow 0$ in Eq. (1), θ_c projects k_c along the asymptotes of the type II hyperbola (Fig. 3(c) inset) where infinitely large wavevectors are supported in the ideal limit. As such, the phase velocity in the medium also approaches 0 at this point ($v_{phase} = \omega/k \rightarrow 0$). The minimum electron velocity where the CR condition is satisfied is as at the point where $v_z = v_{phase}$ and consequently the minimum CR velocity threshold is also $v_{th} \rightarrow 0$ in hyperbolic media.

The electron scattering probability for TCR at different incident electron velocities is plotted in Fig. 3(b) for 60 nm Bi_2Te_3 (with regular damping) in the hyperbolic regime. Due to the hyperbolic topology of Bi_2Te_3 discussed above, the TCR scattering probability increases with decreasing electron velocity. This is the exact opposite trend observed for conventional CR in dielectrics where the CR scattering probability becomes suppressed as v_z decreases. Additionally, the TCR dispersion (Eq. (1)) extends to larger scattering angles (or wavevector, k_c) as the electron velocity is decreased (Fig. 3(c)). Natural hyperbolic media are far more effective at generating TCR than artificial HMMs which are limited by the finite size of their unit cell (d) and can only support wavevector magnitudes reaching the edge of the brillioun zone ($k \approx \pi/d$). This fundamentally limits their ability to reduce the phase velocity (and thus the TCR threshold). However, as natural hyperbolic materials have an atomic sized unit cell, very large magnitudes of k are supported in the structure to achieve TCR with much smaller threshold velocities.

3. Probing high-k modes and hyperbolic CR in Bi_2Te_3 with k-EELS

Figure 4 (a) shows the experimental k-EELS measurements over a range of different scattering angles (momentum) for a 60 nm Bi_2Te_3 film prepared via focused ion beam. Electrons with an energy of 300 keV ($v_z = 0.78c$) are incident on the free-standing sample with a trajectory parallel to the c-axis. Electron scattering angles up to 20 μrad (corresponding to wavevector magnitudes $\approx$ 2-3 times past the free space wavevector $k_0 = \omega/c$) were collected to probe both the high-k modes and the hyperbolic CR mode of Bi_2Te_3.

The experimental k-EELS measurements are plotted as a sum over a range of scattering angles with increasing magnitude as indicated by the 3 curves in Fig. 4(a). The broad peak for all 3 angle sets corresponds to the high-k modes and hyperbolic CR excited in the sample. This is the first measurement of high-k modes probed by k-EELS in any hyperbolic media and the first

Optics EXPRESS

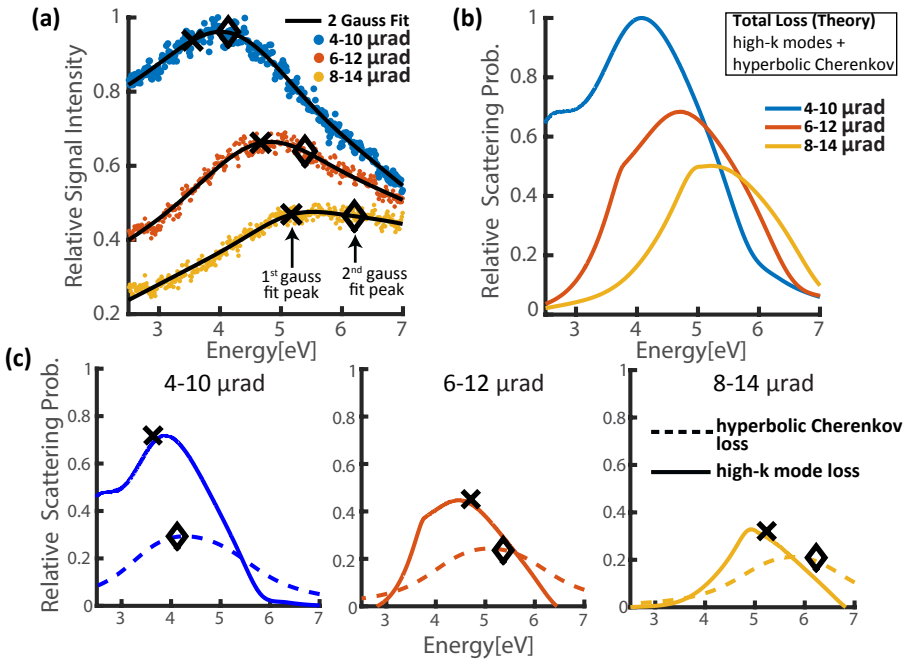

Fig. 4. (a) Experimental energy loss peaks for fast electrons electrons with a velocity of $v_z = 0.78c$ normally incident on the sample of a 60 nm Bi_2Te_3 thin film with no substrate. Three different summed angular ranges of the scattered electrons are shown. The broad peak in each of the 3 sets consist of the high-k modes and the hyperbolic Cherenkov mode. A summation of two gaussian distributions is used to fit the data and the peak positions are marked by crosses and diamonds. (b) Calculated relative electron scattering probability of the total loss in Bi_2Te_3 corroborating the experimental data. (c) The calculated contributions to the total electron scattering probability from the high-k modes and the hyperbolic Cherenkov radiation mode. A strong correlation between the predicted high-k mode and hyperbolic Cherenkov radiation peaks is seen with the gaussian fit peak positions used to fit the experimental data (overlayed cross and diamond).

probe of hyperbolic CR in a natural hyperbolic media. To corroborate our experimental results, the theoretical relative electron scattering probability (equivalent to the relative signal intensity as measured in the experiment) for Bi_2Te_3 is plotted in Fig. 4(b). A strong correlation between the peak positions and the scattering intensity magnitudes is seen between the theory and the experiment. The blue shifting of the energy loss peak with increasing scattering angle in Fig. 4(a) and 4(b) is a result of the dispersive nature of the high-k modes and hyperbolic CR mode (Fig. 2(a)). Note that more conventional EELS techniques would not be able to capture the dispersive nature of such modes but can be captured here by k-EELS. Additionally, the scattering probability in both theory and experiment decreases with increasing scattering angle (as is well known from the inverse scaling of the two parameters [20, 21]).

In Fig. 4(a) a summation of two gaussian distributions are seen to accurately fit the experimental data (black line) for all 3 angle sets. The peak positions of the two separate gaussian distributions are shown as a cross and diamond and correspond to the high-k mode peak and the hyperbolic CR peak, respectively. This is validated in Fig. 4(c) which breaks down the total Bi_2Te_3 loss probability (Fig. 4(b)) into the separate contributions from the high-k modes and the hyperbolic CR mode. The gaussian fit peak positions extracted from experiment (overlayed on the plots) match well with the theoretical predictions for the two predominant peaks. To emphasize, this

Optics EXPRESS

would be the first experimental measurement of the hyperbolic CR mode in natural hyperbolic media and the first measurement by k-EELS of hyperbolic high-k modes.

4. Conclusion

In conclusion, we have performed the first measurement of the hyperbolic CR mode and high-k modes in Bi_2Te_3 with k-EELS. Furthermore, our simulations establish that hyperbolic CR in Bi_2Te_3 can be generated with low electron velocity threshold paving the way for new applications.

Funding

National Science Foundation (NSF) (DMR-1654676).

References

1. R. H. Ritchie, "Plasma Losses by Fast Electrons in Thin Films," Phys. Rev. **106**, 874–881 (1957).
2. F. J. Garcia de Abajo, "Optical excitations in electron microscopy," Rev. Mod. Phys. **82**, 209–275 (2010).
3. J. A. Scholl, A. L. Koh, and J. A. Dionne, "Quantum plasmon resonances of individual metallic nanoparticles," Nature **483**, 421–427 (2012).
4. T. Christensen, W. Yan, S. Raza, A.-P. Jauho, N. A. Mortensen, and M. Wubs, "Nonlocal Response of Metallic Nanospheres Probed by Light, Electrons, and Atoms," ACS Nano **8**, 1745–1758 (2014).
5. P. Shekhar, S. Pendharker, H. Sahasrabudhe, D. Vick, M. Malac, R. Rahman, and Z. Jacob, "Extreme ultraviolet plasmonics and Cherenkov radiation in silicon," Optica **5**, 1590–1596 (2018).
6. S. Molesky and Z. Jacob, "Quantum Optical Sum Rules and Field Fluctuations inside Natural Hyperbolic Media: Hexagonal Boron Nitride and Bismuth Selenide," arXiv, 1702.01862 (2017).
7. X. Yang, J. Yao, J. Rho, X. Yin, and X. Zhang, "Experimental realization of three-dimensional indefinite cavities at the nanoscale with anomalous scaling laws," Nat. Photonics **6**, 450–454 (2012).
8. C. L. Cortes and Z. Jacob, "Super-Coulombic atom-atom interactions in hyperbolic media," Nat. Commun. **8**, 14144 (2017).
9. F. Liu, L. Xiao, Y. Ye, M. Wang, K. Cui, X. Feng, W. Zhang, and Y. Huang, "Integrated Cherenkov radiation emitter eliminating the electron velocity threshold," Nat. Photonics **11**, 289–292 (2017).
10. D. E. Fernandes, S. I. Maslovski, and M. G. Silveirinha, "Cherenkov emission in a nanowire material," Phys. Rev. B **85**, 155107 (2012).
11. J. D. Caldwell, A. V. Kretinin, Y. Chen, V. Giannini, M. M. Fogler, Y. Francescato, C. T. Ellis, J. G. Tischler, C. R. Woods, A. J. Giles, M. Hong, K. Watanabe, T. Taniguchi, S. A. Maier, and K. S. Novoselov, "Sub-diffractional volume-confined polaritons in the natural hyperbolic material hexagonal boron nitride," Nat. Commun. **5**, 5221 (2014).
12. P. Li, M. Lewin, A. V. Kretinin, J. D. Caldwell, K. S. Novoselov, T. Taniguchi, K. Watanabe, F. Gaussmann, and T. Taubner, "Hyperbolic phonon-polaritons in boron nitride for near-field optical imaging and focusing," Nat. Commun. **6**, 7507 (2015).
13. J. Sun, J. Zhou, B. Li, and F. Kang, "Indefinite permittivity and negative refraction in natural material: Graphite," Appl. Phys. Lett. **98**, 101901 (2011).
14. R. Warmbier, G. S. Manyali, and A. Quandt, "Surface plasmon polaritons in lossy uniaxial anisotropic materials," Phys. Rev. B **85**, 085442 (2012).
15. E. E. Narimanov and A. V. Kildishev, "Metamaterials: Naturally hyperbolic," Nat. Photonics **9**, 214–216 (2015).
16. M. N. Gjerding, R. Petersen, T. G. Pedersen, N. A. Mortensen, and K. S. Thygesen, "Layered van der Waals crystals with hyperbolic light dispersion," Nat. Commun. **8**, 320 (2017).
17. P. Shekhar, J. Atkinson, and Z. Jacob, "Hyperbolic metamaterials: fundamentals and applications," Nano Convergence **1**, 1–17 (2014).
18. M. Esslinger, R. Vogelgesang, N. Talebi, W. Khunsin, P. Gehring, S. de Zuani, B. Gompf, and K. Kern, "Tetradymites as Natural Hyperbolic Materials for the Near-Infrared to Visible," ACS Photonics **1**, 1285–1289 (2014).
19. C. H. Chen and J. Silcox, "Calculations of the electron-energy-loss probability in thin uniaxial crystals at oblique incidence," Phys. Rev. B **20**, 3605–3614 (1979).
20. R. Egerton, *Electron Energy-Loss Spectroscopy in the Electron Microscope* (Springer US, 2011).
21. P. Shekhar, M. Malac, V. Gaind, N. Dalili, A. Meldrum, and Z. Jacob, "Momentum-Resolved Electron Energy Loss Spectroscopy for Mapping the Photonic Density of States," ACS Photonics **4**, 1009–1014 (2017).
22. A. Yurtsever, M. Couillard, and D. A. Muller, "Formation of Guided Cherenkov Radiation in Silicon-Based Nanocomposites," Phys. Rev. Lett. **100**, 217402 (2008).
23. I. Frank and I. Tamm, "Coherent Visible Radiation of Fast Electrons Passing Through Matter," in *Selected Papers,* (Springer, Berlin, Heidelberg, 1991), pp. 29–35.
24. J.-K. So, J.-H. Won, M. A. Sattorov, S.-H. Bak, K.-H. Jang, G.-S. Park, D. S. Kim, and F. J. Garcia-Vidal, "Cerenkov radiation in metallic metamaterials," Appl. Phys. Lett. **97**, 151107 (2010).